work and Selig's analytical results[2] that the fluoride analyses were very close to the expected value for $H_3O^+W_2O_2F_9^-$ and that the tungsten analyses fell between the values predicted for $H_2O^+W_2O_2F_9^-$ and $H_3O^+WOF_5^-$.

Since infrared spectra and X-ray diffraction data cannot distinguish easily between H_2F^+ and H_3O^+, another possible hydrolysis product could be $H_2F^+W_2O_2F_9^-$; however, this was ruled out on the basis of the fluoride analysis. As mentioned earlier, the equilibrium between WOF_4 and $W_2O_2F_9^-$ in HF solution strongly favors WOF_4.[13] If $H_2F^+W_2O_2F_9^-$ or WOF_4 was being formed, the Raman spectrum of the HF solution should have shown significant amounts of WOF_4, which would be present as a result of the action of the equilibrium. The $W_2O_2F_9^-$, therefore, must be generated directly from the hydrolysis reaction and not indirectly via the initial formation and reequilibration of WOF_4. This can only occur if a cation is present that is not derived from the solvent. The product, $H_3O^+W_2O_2F_9^-$, suggested by the experimental evidence, is consistent with this requirement.

It has also been proposed[6] that, provided an excess of WF_6 is used, the hydrolysis of WF_6 will yield WOF_4 and that the products, $H_3O^+WOF_5^-$ or $H_3O^+W_2O_2F_9^-$, will only occur in the presence of excess water. The preparation of $H_3O^+W_2O_2F_9^-$ reported here has shown that even with a substantial excess of WF_6 and after several hours reaction time, the hydrolysis product is predominantly $H_3O^+W_2O_2F_9^-$. While the use of excess WF_6 might be expected to favor the formation of WOF_4 on the grounds of stoichiometry, the oxonium adduct is apparently quite stable in HF and is resistant to conversion to WOF_4 by further reaction between H_3O^+ and WF_6.

These results indicate that the controlled hydrolysis of WF_6 and ReF_6 in anhydrous HF is not a viable synthetic route to WOF_4 and $ReOF_4$ although $ReOF_4$ has been reported as the major reaction product when ReF_6 reacts with quartz or glass wool containing small amounts of H_2O or HF.[38] The hydrolysis of MoF_6 in anhydrous HF does, however, readily yield pure $MoOF_4$.

Supplementary Material Available: Listings of thermal parameters, interionic contact distances less than 3.5 Å, and deviations from least-squares mean planes (3 pages); a listing of observed and calculated structure factors (2 pages). Ordering information is given on any current masthead page.

(38) Paine, R. T. *Inorg. Chem.* **1973**, *12*, 1457.

Solubility of Amorphous Chromium(III)–Iron(III) Hydroxide Solid Solutions

Bruce M. Sass[†] and Dhanpat Rai*

Neutralization of acidic solutions containing Cr(III) and Fe(III) at room temperatures results in coprecipitation of these elements as an amorphous solid solution $[Cr_xFe_{1-x}(OH)_3]$. The solubilities of the $Cr_xFe_{1-x}(OH)_3$ precipitates prepared with different mole fractions (x) of $Cr(OH)_3$ (0.99, 0.89, 0.69, 0.49, 0.36, 0.15, 0.09, 0.01, 0.00) were determined in 0.01 M perchlorate solutions between pH 2 and 6 in an N_2 atmosphere. The Cr concentrations in 0.0018-μm filtrates at various times between 5 and 210 days, from initially undersaturated and oversaturated solutions, show that equilibrium was attained within about 7 days when $x < 0.5$ and more slowly when higher mole fractions of $Cr(OH)_3$ were used. In general, aqueous Cr concentrations decrease with decreasing Cr contents in the solids, suggesting that $Cr_xFe_{1-x}(OH)_3$ behaves thermodynamically like a solid solution. Activity coefficients for $Cr(OH)_3$ in the solid solutions were calculated from the solubility data and are given by the equation $\log \lambda_{Cr(OH)_3} = -1.60 + 0.28(1-x)^2 - 1.79(1-x)^3$ for $0.01 \leq x \leq 0.69$. Aqueous Fe activities were generally too low for reliable measurement; therefore, the corresponding activity coefficients for $Fe(OH)_3$ [$\log \lambda_{Fe(OH)_3} = -2.26x^2 + 1.39x^3$] were calculated by a Gibbs–Duhem equation. A general relationship [$\log (CrOH^{2+}) = -2pH + 4.18 + 0.28(1-x)^2 - 1.79(1-x)^3 + \log x$] developed from these data can be used to calculate Cr concentrations in solutions between pH 2 and 6 that are in equilibrium with Cr-bearing ferric hydroxides with known Cr content.

Introduction

To predict maximum elemental concentrations of Cr in groundwaters, thermochemical data are needed for Cr-containing solids that are either initially present or potentially occurring in chemical wastes and in permeable rocks. However, thermochemical data are generally not known for Cr-bearing solids that can form in low-temperature, aqueous environments.

Chromium-bearing solids that can limit groundwater Cr concentrations must have low solubilities and rapid precipitation kinetics. The solid phases that are most likely to control Cr concentrations in surface enviroments are $Cr(OH)_3$ and Cr(III) coprecipitated with Fe oxides.[1] Rai et al.[2] have shown that the precipitation/dissolution kinetics of $Cr(OH)_3$ are rapid and that the solubility between pH 6 and pH 10.5 is very low. However, apart from the observed close association of Cr with iron compounds,[3–5] no quantitative data yet exist for Cr(III) coprecipitated with Fe oxides.

Because Cr^{3+} and Fe^{3+} have like charge and similar ionic radii (0.63 Å and 0.64 Å, respectively[6]), amorphous hydroxide precipitates of these elements at room temperature may behave thermodynamically like true solid solutions. If a solid solution represented by the formula $Cr_xFe_{1-x}(OH)_3$ does form readily at room temperature and has lower solubility than $Cr(OH)_3$, its presence would play an extremely important role in controlling Cr(III) concentrations in groundwaters. The results presented here show that (1) $Cr_xFe_{1-x}(OH)_3$ forms readily at room tem-

(1) Rai, D.; Zachara, J. M.; Schwab, A. P.; Schmidt, R. L.; Girvin, D. C.; Rogers, J. E. "Chemical Attenuation Rates, Coefficients, and Constants in Leachate Migration"; Report EA-3356; Electric Power Research Institute: Palo Alto, CA, 1984; Vol. 1.
(2) Rai, D.; Sass, B. M.; Moore, D. A. *Inorg. Chem.* **1987**, *26*, 345.
(3) Nakayama, E.; Kuwamoto, T.; Tsurubo, S; Fuginaga, T. *Anal. Chim. Acta* **1981**, *131*, 247.
(4) Cranston, R. E.; Murray, J. W. *Anal. Chim. Acta* **1978**, *99*, 275.
(5) Shiraki, K. In *Handbook of Geochemistry*; Wedepohl, K. H., Ed.; Springer-Verlag: Berlin, 1978; Vol. II/3, Part G.
(6) Weast, R. C., Ed. *Handbook of Chemistry and Physics*; The Chemical Rubber Co.: Cleveland, OH, 1984.

†Present address: Department of Chemistry, University of Pennsylvania, Philadelphia, PA 19104-6323.

perature and (2) aqueous Cr in equilibrium with $Cr_xFe_{1-x}(OH)_3$, at the low Cr mole fractions expected in geologic environments, is several orders of magnitude lower in concentration than when in equilibrium with $Cr(OH)_3$.

Materials and Methods

Reagents. Concentrated stock solutions containing different molar proportions of Fe(III)/Cr(III) (approximately 1/99, 1/8, 1/2.2, 1/1, 1.8/1, 5.7/1, 10.1/1, and 99/1) were prepared from $[Cr(H_2O)_4Cl_2]$-$Cl\cdot2H_2O$ (green salt) and $FeCl_3\cdot6H_2O$ in 0.1 M $HClO_4$. The stocks were treated with 30% H_2O_2 (1.6 mL/L stock) at 90 °C to reduce trace amounts of Cr(VI) to Cr(III) and simultaneously oxidize any Fe(II) to Fe(III).

Deionized water was deaerated by boiling and sparged thoroughly at room temperature with an inert gas. Stock solutions of 0.67 M tetra-ethylammonium hydroxide $[(C_2H_5)_4NOH]$ and 10 M NaOH were treated with $BaCl_2$ to remove carbonate and were stored in an inert atmosphere.

General Procedure. Under an inert atmosphere (99.99% N_2 with a few ppm of oxygen), small aliquots of stock solutions containing a total of between 50 and 250 mg of Cr(III) and Fe(III) in different molar proportions were added to polyethylene centrifuge tubes containing about 10 mL of 0.01 M ammonium perchlorate or sodium perchlorate. The pH of these solutions was adjusted to about 9.5 with carbonate-free NaOH or $(C_2H_5)_4NOH$ to coprecipitate Cr(III) and Fe(III); the precipitates are represented by the formula $Cr_xFe_{1-x}(OH)_3$, where x is the mole fraction of $Cr(OH)_3$. After aging for at least 3 h, the suspensions were washed with 0.01 M NH_4ClO_4 or $NaClO_4$ to remove chloride.

Solubility experiments using $Cr_xFe_{1-x}(OH)_3$ and pure $Fe(OH)_3$ (x = 0), prepared by similar means, were conducted in a pH range of approximately 2–6. Experiments were not conducted above neutral pH because pure $Cr(OH)_3$ and $Fe(OH)_3$ are known to have very low solubilities under alkaline conditions. The solubilities of the precipitates were investigated from undersaturation and oversaturation to help determine if equilibrium was attained. To approach the solubility limit from undersaturation, the precipitates were suspended in approximately 30 mL of 0.01 M NH_4ClO_4 or $NaClO_4$ to maintain constant ionic strength, and the suspensions were adjusted to pH values ranging from about 2 to 6 by using $HClO_4$. To approach the solubility limit from oversaturation, the precipitates were dissolved in $HClO_4$, and the solutions (pH <3) were adjusted to higher pH values by using a carbonate-free base. All of the suspensions were continuously agitated on a shaker and equilibrated between 5 and 210 days. At various times, the pH values of the suspensions were measured and aliquots were withdrawn for Cr and Fe analyses.

Measurements. The pH was measured in the suspensions to within 0.01 unit with a Corning 135 pH meter and Ross 81-03 combination glass/reference electrode.

Amicon Centriflo membrane cones (Amicon Corp., Lexington, MA), with approximately 0.0018-μm pore sizes, were shown to be effective in filtering $Cr(OH)_3$ from suspensions without appreciable adsorption of soluble Cr.[2] Therefore, these filters were used for separating solutions from the $Cr_xFe_{1-x}(OH)_3$ suspensions. The 0.0018-μm filtrates were analyzed for Cr and Fe by inductively coupled plasma spectroscopy (Jarrell-Ash 975 Atomcomp) and by atomic absorption spectrophotometry (AAS) (Perkin-Elmer 5000 with graphite furnace). The detection limits by AAS were 2 μg of Cr/L and 10 μg of Fe/L. Some filtrates were also analyzed for Cr(VI) and Fe(II) by visual spectrophotometry,[7-9] but the concentrations of these species were much less than the total Cr and Fe values; hence, they were ignored.

Portions of the solids were occasionally removed, dried at room temperature, and analyzed for crystallinity by X-ray diffraction; all of these solids were found to be amorphous. The molar ratios of Fe/Cr in the solids were determined upon termination of the experiments by separating the solids and dissolving them in nitric acid for analysis. Mole fractions of $Cr(OH)_3$ {x = moles of $Cr(OH)_3$/[moles of $Cr(OH)_3$ + moles of $Fe(OH)_3$]} and $Fe(OH)_3$ were then calculated.

Results and Discussion

For each chemical component in the system $Cr(OH)_3$–$Fe(OH)_3$–H_2O at equilibrium, the chemical potential (μ) must be the same in the solid (s) and aqueous (aq) phases. Thus, $\mu^s_{Cr(OH)_3} = \mu^{aq}_{Cr(OH)_3}$ and $\mu^s_{Fe(OH)_3} = \mu^{aq}_{Fe(OH)_3}$. In the aqueous phase, the dominant species of Cr(III) and Fe(III) are (1) $CrOH^{2+}$ between

(7) Gibbs, M. M. *Water Res.* **1979**, *13*, 295.
(8) Bartlett, R.; James, B. *J. Environ. Qual.* **1979**, *8*, 31.
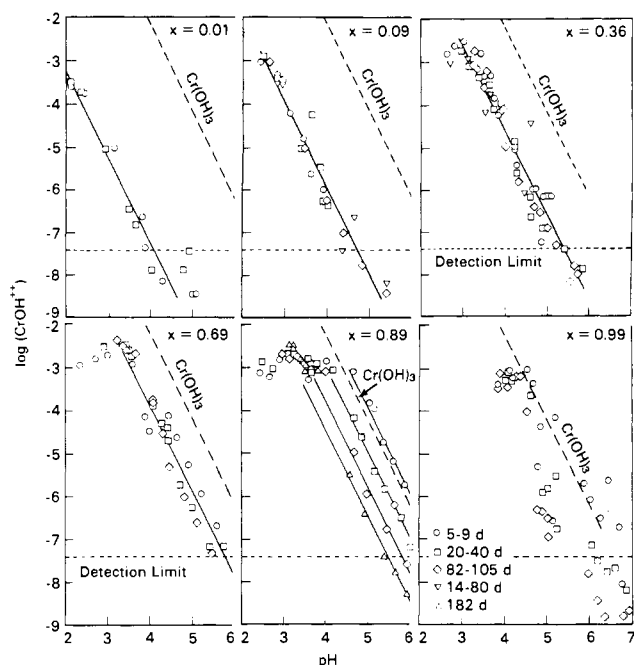(9) Tamura, H.; Goto, K.; Yotsuyanagi, T.; Nagayama, M. *Talanta* **1974**, *21*, 314.

Figure 1. Chromium activities in 0.0018-μm filtrates from suspensions of $Cr_xFe_{1-x}(OH)_3$ [containing different mole fractions of $Cr(OH)_3$ (x); solids with x = 0.15 and 0.49 were also studied but are not reported here] in pH-adjusted 0.1 M NH_4ClO_4 or $NaClO_4$ maintained under an N_2 atmosphere. Solid lines were calculated by linear regression of the data with the constraint that the slopes = -2. At x = 0.89, best-fit lines were calculated for individual times, and for x ⩽ 0.69 all of the data were used in the regressions. The solubility of pure $Cr(OH)_3$ is shown by the dashed lines.[2] Inverted triangles represent equilibrium from the oversaturation direction; all other symbols represent equilibrium from the undersaturation direction.
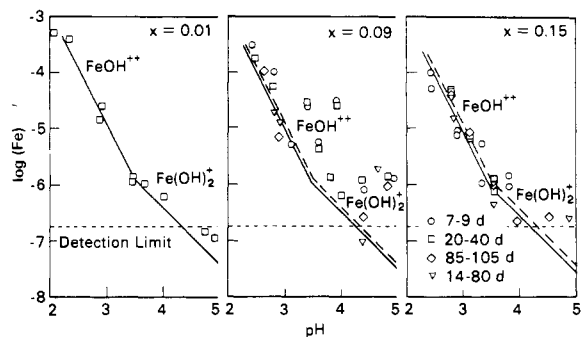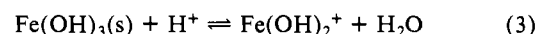

Figure 2. Iron activities in 0.0018-μm filtrates from suspensions of $Cr_xFe_{1-x}(OH)_3$ [containing different mole fractions of $Cr(OH)_3$ (x) between 0.01 and 0.15] in pH-adjusted 0.01 M NH_4ClO_4 or $NaClO_4$ maintained under an N_2 atmosphere. Solid lines indicate the calculated activities of dominent Fe(III) species in solutions that are in equilibrium with $Cr_xFe_{1-x}(OH)_3$, and the dashed lines indicate the solubility of pure $Fe(OH)_3$ (at x = 0.01, these lines overlap). Inverted triangles represent equilibrium from the oversaturation direction; all other symbols represent equilibrium from the undersaturation direction.

pH 3.8 and 6.4[2] (or possibly between pH 2.6 and 6.4[2]), (2) $FeOH^{2+}$ between 2.4 and 3.6,[10] and (3) $Fe(OH)_2^+$ for several pH units above 3.6[10] (all at 0.01 M ionic strength). Equilibrium between $Cr_xFe_{1-x}(OH)_3$ and an aqueous solution in the pH range of interest (approximately 2–6) can be represented by eq 1–3 if the chemical components are in thermodynamic equilibrium.

$$Cr(OH)_3(s) + 2H^+ \rightleftharpoons CrOH^{2+} + 2H_2O \qquad (1)$$

$$Fe(OH)_3(s) + 2H^+ \rightleftharpoons FeOH^{2+} + 2H_2O \qquad (2)$$

$$Fe(OH)_3(s) + H^+ \rightleftharpoons Fe(OH)_2^+ + H_2O \qquad (3)$$

(10) Baes, C. F.; Mesmer, R. E. *The Hydrolysis of Cations*; Wiley: New York, 1976.

To determine whether the results of these experiments are in accord with the equilibrium criteria, the log concentrations of Cr and Fe were plotted against pH; lines that represent eq 1–3 were fitted to the data by least-squares regression. The slopes of the best-fit lines that pertain to eq 1, 2, and 3 are −2, −2, and −1, respectively. These lines were found to adequately represent the solubility data (Figures 1 and 2); hence, no other aqueous species need be considered.

The activities (given by parentheses) of Cr and Fe species were calculated from the total measured aqueous concentrations of Cr and Fe and by using the Davies[11] equation and available hydrolysis constants;[2,10] results are plotted against pH in Figures 1 and 2 at different mole fractions of $Cr(OH)_3$ (x) in the solids. In general, the activities of $CrOH^{2+}$ contacting $Cr_xFe_{1-x}(OH)_3$ in experiments conducted from undersaturation decrease with a decrease in the value of x and with an increase in equilibration time (Figure 1). The solubility of pure $Cr(OH)_3$ is shown for reference. Steady-state activities of $CrOH^{2+}$ appear to have been reached during the course of these experiments for solids with $x \leq 0.69$, but steady-state values were not reached for solids with $x \geq 0.89$. The slope of log ($CrOH^{2+}$) vs. pH, for $x = 0.89$, remains approximately constant at −2, indicating that the decrease in concentration is caused by reduced solubility. The data for $x = 0.99$ are highly variable but also show lower solubility with time. Aging effects are apparently not uniform for the solid denoted by $x = 0.99$. In general, there is good agreement of the results from under- and oversaturation experiments, as indicated in Figure 1 at $x = 0.09$ and 0.36. Nevertheless, the data from all oversaturation experiments were excluded from regression calculations because of potential errors in calculating ionic activities in the higher ionic strength ($\leq$0.4 M perchlorate), oversaturated solutions.

Iron concentrations are near or below detectable levels at pH >4; therefore, only experiments with appreciable data below pH 4 ($x \leq 0.15$) are shown in Figure 2. Because the data for Fe are lacking at intermediate and high Cr contents, the solubility of $Cr_xFe_{1-x}(OH)_3$ will be discussed in terms of the Cr data, and the results will be used to predict aqueous Fe activities, which will be compared with the available experimental data.

The dependence of $CrOH^{2+}$ activities on x is evidence that Fe and Cr are present in a single solid phase, because solubility would not vary as a function of x if the solid were a mixture of discrete $Fe(OH)_3$ and $Cr(OH)_3$ phases. Adsorption of Cr by $Fe(OH)_3$ is probably not an important mechanism for controlling $CrOH^{2+}$ activities because (1) the amount of Cr present in the suspensions, especially for the larger values of x, far exceeds the total number of adsorption sites on $Fe(OH)_3$, (2) the adsorption edge for positively charged $CrOH^{2+}$ should be in the slightly acidic region, but if adsorption is considered to be the controlling mechanism, then the adsorption edge appears to be as low as pH 2, and (3) the change in $CrOH^{2+}$ activity with changes in pH is similar to the change in pure $Cr(OH)_3$ solubility, which suggests solubility, rather than adsorption, phenomena.

When the activity of H_2O is taken to be unity, as is approximately true in dilute electrolyte solutions, equilibrium between $Cr(OH)_3$ and the solution (eq 1) can be expressed by the thermodynamic equilibrium constant

$$K_{s11} = \frac{(CrOH^{2+})}{(H^+)^2 a_{Cr(OH)_3}} \qquad (4)$$

or

$$\log (CrOH^{2+}) = \log K_{s11} - 2pH + \log a_{Cr(OH)_3} \qquad (5)$$

where parentheses represent the activities of the enclosed aqueous species, and $a_{Cr(OH)_3}$ is the activity of $Cr(OH)_3$ in the solid solution. At fixed temperature, pressure, and composition, $a_{Cr(OH)_3}$ is constant if the free energy of the solid is constant. Aging effects will, however, usually lower the free energy of a solid; hence, it is important to determine if equilibrium has been attained before using eq 4 and 5. The value of log K_{s11} was found to be 5.78 ±
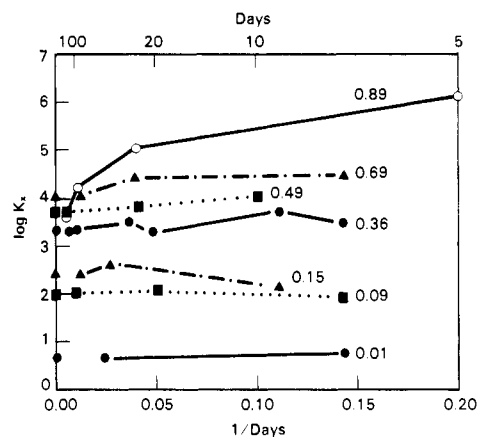
(11) Davies, C. W. *Ion Association*; Butterworths: London, 1962.

Figure 3. log K_x values for the data in Figure 1, representing log $(CrOH^{2+})$ + 2pH at different mole fractions of $Cr(OH)_3$ in $Cr_xFe_{1-x}(OH)_3$, plotted vs. inverse time. Values of log K_x extrapolated to infinite time are shown by the symbols on the ordinate.

Table I. Values of log $K_x{}^a$ Extrapolated to Infinite Time

$x_{Cr(OH)_3}$	log K_x	log $a_{Cr(OH)_3}$	log $\lambda_{Cr(OH)_3}$
1.00	5.78 ± 0.08^b	0.00	0.00
0.69	4.00	−1.78	−1.62
0.49	3.70	−2.08	−1.77
0.36	3.35	−2.43	−1.99
0.15	2.50	−3.28	−2.46
0.09	2.00	−3.78	−2.73
0.01	0.70	−5.08	−3.08

^{a} log K_x = log $(CrOH^{2+})$ + 2pH. ^{b} log K_{s11} value from Rai et al.[2]

0.08 in experiments conducted by Rai et al.[2] with amorphous $Cr(OH)_3$; no change in solubility as a result of aging the solid up to 134 days in acidic solutions was found. Choosing log K_{s11} = 5.78 as the standard-state equilibrium constant for pure, amorphous $Cr(OH)_3$ in equilibrium with $CrOH^{2+}$, one can evaluate the activity of $Cr(OH)_3$ in the solid solutions from

$$\log K_x = \log K_{s11} + \log a_{Cr(OH)_3} \qquad (6)$$

The composition-dependent variable, K_x, equals K_{s11} when $Cr(OH)_3$ is in the standard state; its value when applied to solid solutions of fixed composition can be found by using the relationship obtained by combining eq 5 and 6:

$$\log (CrOH^{2+}) = -2pH + \log K_x \qquad (7)$$

Values of log K_x were calculated by fitting the data in Figure 1 (undersaturation only) at individual equilibration times to curves with a slope of −2 and extrapolating to pH 0; intercepts are shown as a function of inverse time in Figure 3. This empirical treatment shows that, with longer equilibration times, log K_x values do not vary appreciably for $x \leq 0.36$ and decrease slightly for $x \geq 0.49$. Figure 3 also shows that log K_x values generally decrease as x decreases.

Equilibrium values of log K_x were estimated by extrapolating the data in Figure 3 to infinite time; the results are given in Table I. Figure 3 shows that log K_x varies approximately linearly with inverse time for all solid compositions except $x = 0.89$, where the solubility decreases markedly with time. No attempt was made to estimate the equilibrium values of log $K_{0.89}$ and log $K_{0.99}$. The decrease in solubility (log K_x) with time for $x = 0.89$ suggests that solid solutions with large mole fractions of $Cr(OH)_3$ undergo greater structural reorganization after precipitation than do the more Fe-rich solids. Aging effects are apparently not dependent on pH at $x = 0.89$, because even where solubility varies considerably with time (Figure 1, $x = 0.89$), the data can still be plotted on curves with slope of −2, indicating that the free energy of the solid is constant during the experiments.

The equilibrium solubilities of $Cr_xFe_{1-x}(OH)_3$ at several compositions were calculated by using the equilibrium values of log K_x and are illustrated in Figure 4. The solubilities of the solid
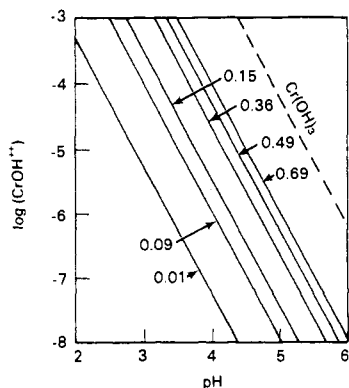
Figure 4. Equilibrium $CrOH^{2+}$ activities in contact with $Cr_xFe_{1-x}(OH)_3$. The solid lines were calculated from log K_x values that were extrapolated to infinite time (Table I). The dashed line represents the solubility of pure $Cr(OH)_3$.[2]
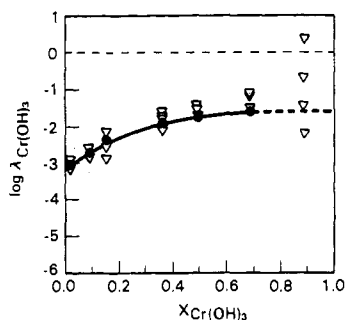

Figure 5. Logarithmic activity coefficients of $Cr(OH)_3$ in $Cr_xFe_{1-x}(OH)_3$ at different $Cr(OH)_3$ mole fractions. Inverted triangles show values calculated at various times. The smoothed curve was determined by least-squares regression of the equilibrium data points (filled circles).

solutions are all much less than the solubility of pure $Cr(OH)_3$ and decrease as the Cr content in the solid decreases. A relatively large difference exists between the solubility of pure $Cr(OH)_3$ and the Cr-rich solid solution ($x = 0.69$). Moreover, the trend does not suggest that solids with higher Cr contents would approach the solubility of pure $Cr(OH)_3$, and attempts to experimentally determine the solubilities of Cr-rich solid solutions were inconclusive because these solids reach equilibrium much more slowly than the Fe-rich members (Figure 3).

The activities of $Cr(OH)_3$ in the solids were calculated by subtracting 5.78 (log K_{s11}) from log K_x values (see eq 6); estimates of the equilibrium activities are given in Table I. Activity coefficients (λ) were calculated from activity and composition data by using

$$a_{Cr(OH)_3} = x\lambda_{Cr(OH)_3} \qquad (8)$$

Values of log $\lambda_{Cr(OH)_3}$ are plotted in Figure 5 as a function of x at different times (inverted triangles). The dependence of log $\lambda_{Cr(OH)_3}$ on x, from the extrapolated log K_x values (filled circles), was calculated by least-squares polynomial regression (for $0.01 \leqslant x \leqslant 0.69$) and has the form

$$\log \lambda_{Cr(OH)_3} = -1.60 + 0.28(1 - x)^2 - 1.79(1 - x)^3 \quad (9)$$

The activity coefficients for $Cr(OH)_3$ are much less than 1, indicating highly favorable mixing properties.

The large difference in log $\lambda_{Cr(OH)_3}$ between the observed value of -1.62 at $x = 0.69$ and the theoretical value of zero at $x = 1$ (Figure 5) may reflect a change in the $Cr(OH)_3$ structure when Fe(III) is present. This phenomenon can also be observed in Figure 4, where the solubility curves do not vary continuously up to that of pure $Cr(OH)_3$ but become "compressed" as x approaches 0.69.

If $Cr_xFe_{1-x}(OH)_3$ is a true solid solution, the activity of the $Fe(OH)_3$ component should also vary with solid composition. Unfortunately, $Fe(OH)_3$ activities cannot be evaluated throughout the entire compositional range of $Cr_xFe_{1-x}(OH)_3$, because accurate,

aqueous Fe concentrations could only be measured in solutions contacting relatively Fe-rich solid solutions. If, however, $Cr(OH)_3$ and $Fe(OH)_3$ are in thermodynamic equilibrium with their respective components in the aqueous phase, as the data for $Cr(OH)_3$ solubilities indicate, they must be related to one another by a Gibbs–Duhem equation. Then, at constant temperature and pressure, the following relationship exists between the activity coefficients of the components in the solid solution:

$$\frac{d}{dx} \log \lambda_{Fe(OH)_3} = \left(\frac{-x}{1-x}\right)\left(\frac{d}{dx} \log \lambda_{Cr(OH)_3}\right) \qquad (10)$$

Substituting eq 9 into eq 10 and integrating yield

$$\log \lambda_{Fe(OH)_3} = -2.41x^2 + 1.79x^3 \qquad (11)$$

The convention that $\lambda_{Fe(OH)_3} = 1$ at $x = 0$ was used in evaluating eq 11.

The activity of $Fe(OH)_3$ at any composition, x, can be calculated by combining eq 8 and 11. Activities of Fe(III) species in equilibrium with $Cr_xFe_{1-x}(OH)_3$ can then be determined by using hydrolysis data for Fe(III)[10] and solubility data for pure $Fe(OH)_3$ (this study). The solubility curves in Figure 2 were thus calculated by

$$\log (FeOH^{2+}) =$$
$$-2pH + 1.06 - 2.41x^2 + 1.79x^3 + \log (1 - x) \quad (12)$$

$$\log (Fe(OH)_2^+) =$$
$$-pH - 2.42 - 2.41x^2 + 1.79x^3 + \log (1 - x) \quad (13)$$

Although the predicted solubility curves for the solid solutions differ only slightly from those for pure $Fe(OH)_3$, the fact that the predicted curves are consistent with the experimental data suggests that the solid-solution model is correct.

The mixing properties of nonelectrolyte solutions are frequently described in terms of Henry's and Raoult's laws. According to Henry's law, the activity coefficient of the minor component approaches a constant value at high dilutions. This behavior is not observed for $Cr(OH)_3$ because the derivative, d log $\lambda_{Cr(OH)_3}$/dx, is positive at low values of x (see Figure 5). Raoult's law behavior, for which the activity coefficient of the major component approaches unity as the phase becomes pure with respect to that component, cannot be tested for $Cr(OH)_3$-rich solid solutions because of the uncertainty in the data at $x > 0.69$. Theoretically, the log $\lambda_{Cr(OH)_3}$ curve must have zero slope and a value of zero in the limit as $x = 1$. The discontinuity in log $\lambda_{Cr(OH)_3}$ at $x > 0.69$ is probably caused by a large difference between the free energy of the pure solid and that of the solid solution. Small activity coefficients for $Cr(OH)_3$ indicate that mixing enthalpies are highly exothermic, which usually means that attractive forces are greater (the bonds are stronger) between unlike component molecules than between like components.[12] Thus, the solubility of Cr-rich $Cr_xFe_{1-x}(OH)_3$ is markedly reduced relative to that of pure $Cr(OH)_3$. Similar behavior is not observed for high $Fe(OH)_3$ concentrations. Small additions of $Cr(OH)_3$ to $Fe(OH)_3$ result in small negative values for log $\lambda_{Fe(OH)_3}$. Apparently the structure of amorphous $Fe(OH)_3$ is less affected by the addition of $Cr(OH)_3$ than the converse.

Because apparent equilibrium solubilities of $Cr_xFe_{1-x}(OH)_3$ were obtained between $x = 0.01$ and $x = 0.69$, which do not extrapolate to the solubility of pure $Cr(OH)_3$ (see Figure 5), a different standard state of $Cr(OH)_3$ was chosen to be in accord with the apparent equilibrium data and Henry's law. The trend of the log $\lambda_{Cr(OH)_3}$ curve in Figure 5 suggests that the activity coefficients are approaching a constant value at approximately $x = 0.69$. Therefore, the curve, log $\lambda_{Cr(OH)_3}$, was extrapolated to $x = 1$ with the constraint that the slope equal zero at $x = 1$ (dashed curve in Figure 5), and the activity coefficient was redefined to be unity at $x = 1$. This hypothetical standard state differs from the previous definition where $K_{1.00} = K_{s11}$; hence, $Cr(OH)_3$ represented by the

(12) Swalin, R. A. *Thermodynamics of Solids*, 2nd ed.; Wiley: New York, 1972.

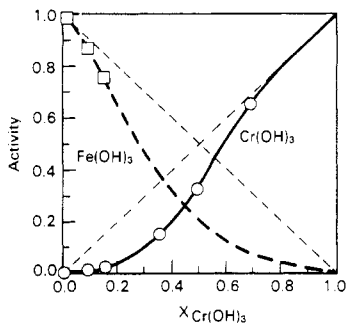**Figure 6.** Activities of $Cr(OH)_3$ and $Fe(OH)_3$ in $Cr_xFe_{1-x}(OH)_3$. The solid curve was obtained by least-squares regression of the equilibrium $Cr(OH)_3$ activity coefficients (Table I) (circles) for the hypothetical standard state of $Cr(OH)_3$ (see eq 14). The corresponding activities of $Fe(OH)_3$ (dashed curve) were calculated by a Gibbs–Duhem equation; squares indicate the $Fe(OH)_3$ activities in Figure 2.

hypothetical state is not physically equivalent to freshly precipitated $Cr(OH)_3$. Activity coefficients for $Cr(OH)_3$ based on the hypothetical standard state ($\lambda^*_{Cr(OH)_3}$) are given by

$$\log \lambda^*_{Cr(OH)_3} = 0.28(1 - x)^2 - 1.79(1 - x)^3 \qquad (14)$$

The standard state of $Fe(OH)_3$ remains unchanged as the pure amorphous solid precipitated by the methods described earlier.

Activities of $Cr(OH)_3$ and $Fe(OH)_3$, based on eq 11 and 14, are shown in Figure 6. The shapes of the activity curves suggest that $Cr_xFe_{1-x}(OH)_3$ behaves like a typical solution that deviates negatively from an ideal mixture.

Conclusions

Solids containing different proportions of Cr(III) and Fe(III) were precipitated by $(C_2H_5)_4NOH$ or NaOH and equilibrated in 0.01 M perchlorate solutions between pH 2 and 6 in an N_2 atmosphere. Experiments were performed at different time periods and from under- and oversaturation and indicate that equilibrium was attained or could be estimated for solid compositions with less than about 70 mol % $Cr(OH)_3$.

In general, Cr contents in the 0.0018-μm filtrates decrease with a decrease in the mole fraction of $Cr(OH)_3$ in the solid (x). Activity coefficients for $Cr(OH)_3$ (solid) are much less than 1 at most of the investigated compositions ($x \leqslant 0.89$), indicating that mixing with $Fe(OH)_3$ is highly favorable. Activity coefficients for $Fe(OH)_3$ (solid) were calculated by using a Gibbs-Duhem equation and provide results that are consistent with the observed aqueous Fe activities in solutions contacting solids with values of $x \leqslant 0.15$. The results of these experiments support the hypothesis that coprecipitated $Cr(OH)_3$ and $Fe(OH)_3$ behave thermodynamically like solid solutions.

A composition-dependent solubility equation can be derived from the equations presented here and can be used to predict aqueous Cr concentrations in equilibrium with $Cr_xFe_{1-x}(OH)_3$. For $x \leqslant 0.69$ and for pH between 2 and 6, the following equation is valid:

$$\log (CrOH^{2+}) =$$
$$-2pH + 4.18 + 0.28(1 - x)^2 - 1.79(1 - x)^3 + \log x \quad (15)$$

Equation 15 is applicable to natural systems where the Fe-(III)/Cr(III) ratio is high.

Contribution from the Department of Chemistry,
University of Michigan, Ann Arbor, Michigan 48109

Boron Nuclear Quadrupole Coupling in Trimethylphosphine–Borane

Kurt W. Hillig, II, and Robert L. Kuczkowski*

The hyperfine splitting due to the boron nuclear electric quadrupole moment was measured in trimethylphospine–borane by Fourier transform microwave spectroscopy techniques. The coupling constant, $eQq = 1.198$ (20) MHz, was interpreted in terms of the fractional number of electrons donated from phosphorus to boron. A value of 0.61 was estimated. The results were compared with coupling constants for methylphosphine–borane and trifluorophosphine–borane.

The development of high-resolution Fourier transform microwave (FTMW) spectroscopy has led to the determination of boron nuclear quadrupole coupling constants in two phosphine–borane adducts, $PF_3 \cdot BH_3$[1] and $CH_3PH_2 \cdot BH_3$.[2] It is well-known that quadrupole coupling constants can give information about the electron distribution about boron.[3-5] This motivated us to undertake a similar analysis of $(CH_3)_3P \cdot BH_3$ in order to make comparisons among these systems. The microwave spectrum of $(CH_3)_3P \cdot BH_3$ had been previously investigated and structural parameters were determined, but the boron quadrupole splitting was not resolved.[6]

Experimental Section

The sample preparation has been described elsewhere.[6] The spectrum was observed with a FTMW spectrometer described in another report.[7] A heated pulsed supersonic nozzle was used to produce a molecular beam to minimize collisional broadening of the transitions. This was made by adding a small heated stainless-steel chamber containing a few tenths of a gram of solid to a modified Bosch fuel injector valve.[8] The carrier gas moving slowly through the chamber became saturated at the equilibrium

(1) Kasten, W.; Dreizler, H.; Kuczkowski, R. L. *Z. Naturforsch., A: Phys., Phys. Chem., Kosmophys.* **1985,** *40A,* 920.
(2) Kasten, W.; Dreizler, H.; Kuczkowski, R. L.; Labarge, M. S. *Z. Naturforsch., A: Phys., Phys. Chem., Kosmophys.* **1986,** *41a,* 835.
(3) Townes, C. H.; Schawlow, A. L. *Microwave Spectroscopy*; McGraw-Hill: New York, 1955.
(4) Gordy, W.; Cook, R. L. *Microwave Molecular Spectra*; Wiley: New York, 1984.
(5) Lucken, E. A. C. *Nuclear Quadrupole Coupling Constants*; Academic: New York, 1969.

(6) Bryan, P. S.; Kuczkowski, R. L. *Inorg. Chem.* **1972,** *11,* 553.
(7) Hillig, K. W.; Matos, J.; Scioly, A.; Kuczkowski, R. L. *Chem. Phys. Lett.* **1987,** *133,* 359.
(8) Otis, C. E.; Johnson, P. M. *Rev. Sci. Instrum.* **1980,** *51,* 1128.